

# Multi-UAV Pre-positioning and Routing for Power Network Damage Assessment

Gino J. Lim, *Member, IEEE*, Seonjin Kim, Jaeyoung Cho, Yibin Gong, and Amin Khodaei, *Member, IEEE*

**Abstract**— This paper presents a two-phase mathematical framework for efficient power network damage assessment using unmanned aerial vehicle (UAV). In the first phase, a two-stage stochastic integer programming optimization model is presented for damage assessment in which the first stage determines the optimal UAV locations anticipating an arrival of an extreme weather event, and the second stage is to adjust the UAV locations, if necessary, when the arrival time of the predicted extreme weather becomes closer with updated information. UAV paths to scan the power network are generated in the second phase to minimize operating costs and final damage assessment completion time of the UAVs. Computational techniques are developed to help reduce the solution time. Numerical experiments show that the proposed stochastic model outperforms the deterministic counterpart in terms of the total UAV pre-positioning setup cost. Additionally, sensitivity analysis discovered the relations among damage assessment time, UAV pre-positioning setup cost, and operating cost.

**Index Terms**—UAV, stochastic programming, power network, damage assessment.

## NOMENCLATURE

$G(V, E)$	Directed network with nodes $V$ and edges $E$
$V$	Set of nodes $V = \{1, 2, 3, \dots, i\}$
$V_1$	Set of target nodes where $V_1 \subseteq V$
$V_2$	Set of UAV pre-positioning candidates where $V_2 \subseteq V$ and $V_1 \cap V_2 = \emptyset$
$V_{21}$	Set of UAV pre-positioning candidates connected to edge(s) in a network where $V_{21} \subseteq V_2$
$V_{22}$	Set of UAV pre-positioning candidates disconnected to edge(s) in a network where $V_{22} \subseteq V_2$ and $V_{21} \cap V_{22} = \emptyset$
$V'$	Set of selected UAV pre-positioning locations where $V' \subseteq V_2$
$J$	Set of revised target nodes for Phase 2 where $J = V_1 \cup (V_{21} - V')$
$E$	Set of edges $E = \{(i, j): i, j \in J, i \neq j\}$
$E_1$	Set of initial routes from a UAV pre-positioned location to a target node $E_1 = \{(i, j): i \in V', j \in J\}$ , where $E_1 \subseteq E$
$E_2$	Set of intermediate routes from a target node to another target node $E_2 = \{(i, j): i, j \in J\}$ where

$E_3$	Set of returning routes from a target node to a pre-positioning location $E_3 = \{(i, j): i \in J, j \in V'\}$ where $E_3 \subseteq E$ , $E_1 \cap E_2 \cap E_3 = \emptyset$ and $E_1 \cup E_2 \cup E_3 = E$
$K$	Set of UAV IDs $K = \{1, 2, 3, \dots, k\}$
$\Omega$	Set of sample scenarios of extreme weather events $\omega \in \Omega$
$c_i$	Unit setup cost for UAV pre-positioning location at $i \in V_2$ in the 1 <sup>st</sup> stage
$c_i^+$	Unit setup cost for UAV pre-positioning location at $i \in V_2$ in the 2 <sup>nd</sup> stage
$\overline{ppl}$	Maximum number of UAV pre-positioning locations can be installed in the 2 <sup>nd</sup> stage
$a_{i,j,\omega}$	1 if an edge $(i, j) \in E_1$ is within the service range and a pre-positioning location candidate $i$ can endure the impact of weather condition $\omega \in \Omega$ and 0 otherwise
$d_{i,j}$	UAV travel time (min.) over edge $(i, j) \in E$
$c_k^{dep}$	Deployment cost of UAV $k \in K$
$FT$	Final damage assessment completion time
$\lambda$	A weight factor in the bi-objective function
$B_k$	Maximum flight time (min.) of UAV $k \in K$
$ST_j$	Node scanning time at $j \in V_1$
$y_i$	1 if UAV pre-positioning location $i \in V_2$ is selected and 0 otherwise
$x_{i,j,k}$	1 if UAV $k \in K$ traverse over an edge $E(i, j)$ and 0 otherwise
$h_k$	1 if UAV $k \in K$ is mobilized and 0 otherwise
$\widetilde{ad}_i^+$	1 if UAV pre-positioning location candidate $i \in V_2$ is selected in the 2 <sup>nd</sup> stage and 0 otherwise
$ad_{i,\omega}^+$	1 if UAV pre-positioning location candidate $i \in V_2$ is selected in the 2 <sup>nd</sup> stage according to a sample scenario $\omega \in \Omega$ and 0 otherwise
$drb_i$	Durability scale of pre-positioning location candidate $i \in V_2$ ; $0 \leq drb_i \leq 1$
$wx_\omega$	Impact scale of an extreme weather according to a sample scenario $\omega \in \Omega$ ; $0 \leq wx_\omega \leq 1$
$P$	Probability of extreme weather events; $0 \leq P \leq 1$
$u_i$	The order of sequence of visiting node $i \in V_1$ in a path

The statements made herein are solely the responsibility of the authors.

Gino J. Lim, and Seonjin Kim are with the Department of Industrial Engineering, University of Houston, TX 77204 USA (e-mail: [ginolim@uh.edu](mailto:ginolim@uh.edu); [skim72@uh.edu](mailto:skim72@uh.edu)). Jaeyoung Cho is with the Department of Industrial

Engineering, Lamar University, TX 77710 (e-mail: [uncmac.rokag@gmail.com](mailto:uncmac.rokag@gmail.com)), Amin Khodaei is with the Department of Electrical and Computer Engineering, University of Denver, CO 80210 USA (e-mail: [amin.khodaei@du.edu](mailto:amin.khodaei@du.edu)).

## I. INTRODUCTION

IN January 2016, winter storm Jonas overwhelmed United States and paralyzed major urban functions in the mid-Atlantic and East Coast. Especially heavy snow and strong winds knocked out power to hundreds of thousands of people along East Coast for a considerable period of time. However, it was only one of the many extreme weather events that happen every year with different levels of undesired aftermath. Extreme weather events and natural disasters can cause tremendous damage over a large geographical area that can stretch to hundreds of miles, while limiting repair crews' access to the damaged areas [1, 2]. Power outage as one of the biggest disruptions causes many further problems because people are usually unprepared, and also unaware about the true impacts that can rapidly influence telecommunication networks, healthcare systems, water supplies and financial services as time goes.

It is clear that improving the estimated time of restoration (ETR) is a high contributing factor for a successful power network recovery to minimize losses and potential risks. However, less than 20 percent of utility companies can complete infrastructure damage assessment on time without delaying expected repair schedule according to a survey [3, 4].

Majority of utility companies have used helicopters for aerial reconnaissance, such as annual transmission overhead power lines inspections, and low-definition post-disturbance inspections in wide area [5]. Helicopter inspection at stand-off range can speed up disaster damage assessment but cannot ensure high quality information. To obtain high-definition information while maintaining advantages of aerial reconnaissance by helicopter, unmanned aerial vehicles (UAVs) can be utilized for damage assessment. Unlike manned aerial vehicles, UAVs can fly autonomously or be piloted remotely, and can get closer to damaged infrastructures for precision scanning. UAV reconnaissance has an advantage in terms of cost-effectiveness compared to helicopter inspection. Therefore, UAV inspection is mostly likely to be a common way of damage assessment in the near future.

Electric Power Research Institute (EPRI) had successfully conducted an experiment with two types of UAVs up to an altitude of 100 feet to evaluate large scale storm damages in 2013. It was verified that operating UAVs with thermal FLIR camera, CCTV camera, and GPS can scan over power networks in a close distance, and can transmit damage information to a ground control center to confirm the degree of damages for restoration planning.

There has been an increasing trend of research on efficient power network design, defense and damage assessment. Power networks as a critical infrastructure require highly reliable protection measures against terror attacks and natural disasters. Interdiction strategy identification method, bi-level or tri-level defender-attacker-defender models and solution algorithms have been reported for an optimal resource allocation to defend critical infrastructures [6, 7, 8, 9]. The resilient distribution network design and planning problem against natural disasters have also been noted as critical challenges [10, 11].

As power network damage assessment environment is very dangerous, autonomous systems such as robots, automated helicopters, and UAVs are suggested to secure the safety of inspection workers. Majority of these studies have mainly focused on equipment design, system dynamics, and control problems [12, 13, 14].

Considerable body of work on a large number of UAVs has been done including topics such as coordination between multiple UAV operators [15], future position prediction [16], air traffic flow optimization [17, 18], and routing optimizations [19, 20]. Especially mathematical optimization models for multiple UAV task assignment and path planning have studied considering technical specifications and operational constraints including mission types, time limits, and no fly zones [21, 22, 23, 24, 25]. This problem has the structure of multiple vehicles routing problem, and tried to solve either by exact algorithms or approximation algorithms [26, 27, 28, 29].

This study is about the use of UAVs for the power network damage assessment problem. Within the scope, the proposed concept is to utilize multiple UAVs to accelerate the inspection speed considering the random realization of an extreme weather event. Some related research works have mainly focused on visiting target nodes using multiple UAVs [30, 31]. However, those approaches did not consider scanning both connected edges (powerline) and nodes (power bus) together in the model as we discuss in this paper.

The literature review reveals that there is no mathematical model specifically developed to employ a fleet of UAVs for power network damage assessment considering uncertainty in weather forecast even though a relatively large volume of research has been conducted in the area of a single UAV inspection. Therefore, a new mathematical framework is proposed in this paper to find optimal pre-positioning locations and paths for multiple UAVs to cover the whole target nodes and edges considering uncertainty in the weather information. The contributions of the paper are listed as follow:

- A new power network damage assessment concept and procedure is developed to minimize overall inspection time and cost. The proposed approach begins by positioning a certain number of UAVs in pre-determined points over the weather impact zone before an expected event. After the extreme weather, pre-positioned UAVs maneuver over the network in accordance with the optimized scanning paths.
- A two-phase mathematical optimization model is proposed for multi-UAV pre-positioning and routing for power network damage assessment (MUAV). In Phase 1 (MUAV-ph1), the optimum UAV positions are found. The MUAV-ph1 is formulated as a two-stage stochastic integer program, where the first stage decision assigns each UAV position and the second stage augments additional UAV positions in accordance with updated weather forecast. In Phase 2 (MUAV-ph2), UAV scanning paths are generated while minimizing UAV operating cost and inspection completion time.
- Computational techniques have been suggested, including constraints reformulation, probing-based preprocessing techniques, logical inequality, and

Lagrangian methods, to enhance the computational performance.

The rest of the paper is organized as follows. Section II describes the problem of power network damage assessment using multiple UAVs. Section III presents the mathematical formulations for MUAV and computational considerations. Section IV discusses computational results. The paper is concluded with discussions of opportunities for extensions of the proposed work in Section V.

## II. PROBLEM STATEMENT AND MODEL OUTLINE

The MUAV problem objective is to provide optimal positions of UAVs and their associated flying paths for an expedited damage assessment. Operating UAVs must be able to scan all designated target nodes and edges while minimizing completion time and total cost for multiple UAVs mobilization.

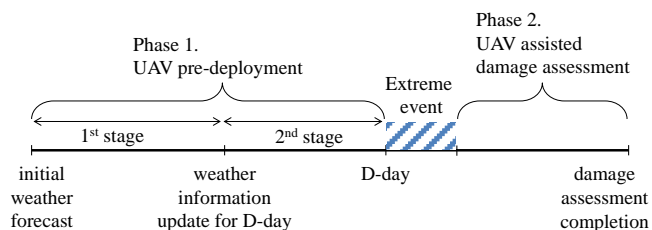


Fig. 1. Power network damage assessment over a planning horizon

Fig. 1 presents a power network damage assessment planning procedure over a planning horizon. If we consider that UAVs are pre-positioned closer to a potential impact area before a disaster strikes the region, damage assessment can be expedited as pre-positioned UAVs immediately collect and transmit the assessment information as soon as the event gets cleared. Consequently, a fast recovery plan can be developed and its implementation will be accelerated.

Therefore, the first phase starts from determining UAV pre-positioning locations among multiple candidates to cover all target facilities while minimizing the number of UAV positions and its cost. As new technologies enable more precise forecast of extreme weather conditions, a better prediction of an impact due to such an event can be made as the arrival time of the event becomes closer. If UAV positions are determined only after accurate weather information is available, UAVs can be placed just around the perimeter of the impending disaster impact area; hence, it can greatly help assess damage soon after the disaster. However, it is likely that there may not be enough time to complete UAV positioning if we delay too long because the roads can be potentially congested as residents started evacuation and also other resources are deployed for pre-planned risk mitigation activities. On the other hand, if UAV positions are determined well in advance, the variance of the forecast error can be high. As a result, some pre-positioned UAV locations can be far out of the weather impact zone that may require repositioning after the event. Therefore, our goal in this paper is to address these issues by decomposing the problem into two stages. In the first stage, UAV pre-positioning locations are selected anticipating an arrival of an extreme weather. The second stage is to adjust the UAV locations, if

necessary, when the arrival time of the predicted extreme event becomes closer with updated weather forecast.

The second phase is to determine the optimal number/type/location of UAVs to generate optimal UAV paths to complete damage assessment in a minimal time. No on-site crews are required for the mission and multiple UAVs can be placed at each pre-positioning locations. Furthermore, both UAV deployment cost and assessment completion time are considered in our optimization model.

For the path planning, every path has to follow four requirements: i) UAV traverses directly from depot to any accessible target node; ii) Each target node and edge is scanned only once but can be visited multiple times to pass through; iii) UAV returns either to the original position or another depot; and, iv) Every deployed UAV conducts a single damage assessment flight along the designated flight path.

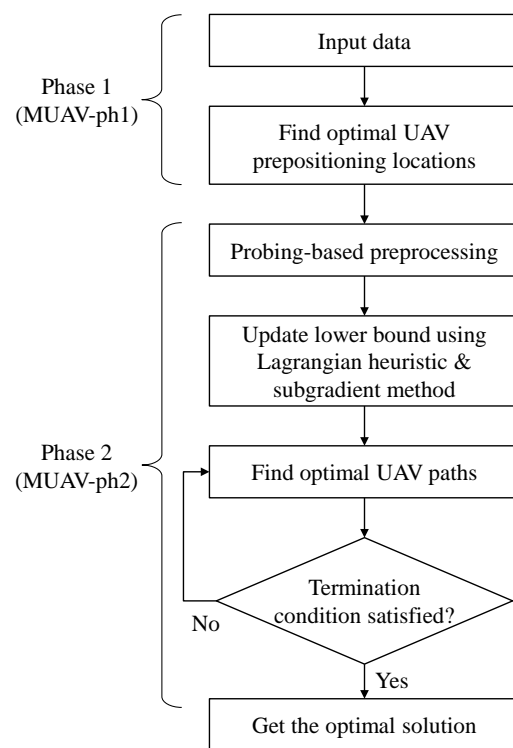


Fig. 2. Flowchart of optimization of MUAV model

Fig. 2 depicts the flowchart of the proposed two-phase optimization of MUAV problem. The Phase 1 problem is formulated as a two-stage stochastic integer program whose goal is to determine UAV pre-positioning locations. Input data to the model include UAV maximum flight time, facility durability scale, and extreme weather impact scale which is random. The Phase 2 problem generates UAV paths for post-disaster damage assessment. Once UAV location information is given to MUAV-ph2, a probing-based preprocessing method eliminates infeasible edges considering UAV flight capacity, and calculates upper bounds for target coverage constraint. A Lagrangian heuristic and a subgradient method [32] are applied to obtain a tight lower bound on the optimal value of MUAV-ph2.

### III. MATHEMATICAL FORMULATION

MUAV is modeled on a directed network  $G(V, E)$  which is composed of two types of nodes and three types of edges: target node set  $V_1$ , UAV pre-positioning location set  $V_2$ , initial route set  $E_1$ , intermediate route set  $E_2$ , and return route set  $E_3$ . The UAV position set  $V_2$  is divided into two subsets: (1) a set of nodes connected with edge(s) in the impacted area  $V_{21}$  and (2) all other nodes  $V_{22}$ . For example, as illustrated in Fig. 3, a power network has two target nodes  $n_1, n_2 \in V_1$  and four UAV pre-positioning candidate points, where  $n_3, n_4 \in V_{21}$ ,  $n_5, n_6 \in V_{22}$ .

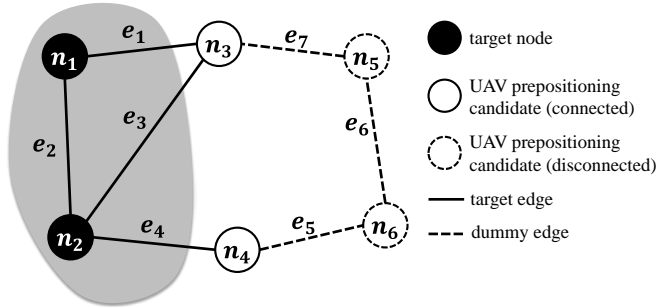


Fig. 3. An illustrative example of a power network

#### A. Phase1: UAV Pre-positioning (MUAV-ph1)

Phase 1 model determines which UAV pre-positioning locations are to setup so as to assess all target nodes and edges considering weather uncertainty. We formulated it as a two-stage stochastic program, MUAV-ph1. Due to the stochastic property of weather information, determining pre-positioning locations in MUAV-ph1 are computationally challenging. Therefore, we approximated the solution by a deterministic equivalent of MUAV-ph1, and solved the model by taking sample scenarios  $\omega^1, \dots, \omega^N \sim P$ . The optimization formulation is as follows:

$$\min \sum_{i \in V_2} c_i y_i + \frac{1}{|\Omega|} \sum_{i \in V_2} \sum_{\omega \in \Omega} c_i^+ ad_{i,\omega}^+, \quad (1)$$

$$s. t. \sum_{i \in V_2} a_{i,j,\omega} (y_i + ad_{i,\omega}^+) \geq 1, \quad (2)$$

$$y_i + ad_{i,\omega}^+ \leq 1, \quad \forall j \in V_1, \omega \in \Omega, \quad \forall i \in V_2, \omega \in \Omega, \quad (3)$$

$$\sum_{i \in V_2} ad_{i,\omega}^+ \leq \overline{ppl}, \quad \omega \in \Omega. \quad (4)$$

The objective function (1) is to minimize the overall pre-positioning location setup cost. The first term is the sum of costs for UAV location setups in the 1<sup>st</sup> stage. The second term is the approximated sample average of all scenarios considered for additional position setups that replaces the typical expectation term,  $E_P[\sum_{i \in V_2} c_i^+ \widetilde{ad}_i^+]$ . Constraint (2) ensures that a target edge must be covered by at least one UAV pre-positioning location. The value of  $a_{i,j,\omega}$  in (2) is determined based on two

criteria: First, every powerline and power bus must be covered by selected UAV pre-positioning locations. As described in the first condition of Algorithm 1, a UAV pre-positioning location is selected only if (1) an UAV can cover at least one transmission line; and (2) it can complete the damage assessment flight by landing at any adjacent UAV pre-positioning location considering the maximum flight range of an UAV. Second, pre-positioning location must be durable enough to withstand the impact of a random extreme weather disruption. If both conditions are satisfied, then  $a_{i,j,\omega}$  becomes 1 and 0 otherwise.

#### Algorithm 1: Determination of $a_{i,j,\omega}$

```

for  $i, i' \in V_2, j, l \in V_1, k \in K, \omega \in \Omega$  do
  if
     $\left\{ \begin{aligned} &(d_{i,j} + ST_j + \max\{d_{j,l} + ST_l + \min\{d_{l,i'}\}\} \leq \min\{B_k\}) \right. \\ &\text{and } (drb_i > wx_\omega) \end{aligned} \right\}$ 
  then
     $a_{i,j,\omega} = 1$ 
  else
     $a_{i,j,\omega} = 0$ 
  end if
end for

```

Constraint (3) controls that any chosen pre-positioning location is set up either in the 1<sup>st</sup> stage or in the 2<sup>nd</sup> stage. Constraint (4) limits the maximum number of UAV positions in the 2<sup>nd</sup> stage considering availability of resources for the UAV pre-positioning tasks.

After the selection of UAV pre-positioning locations by MUAV-ph1, the remaining unselected nodes are re-labeled as dummy nodes, and then input again for UAV paths generation in MUAV-ph2. As shown in Fig. 3,  $e_4$  is a target edge which requires damage assessment. Suppose that node  $n_4$  is not selected as a pre-positioning location in Phase 1. Then,  $n_4$  will be excluded from the network in Phase 2. But, edge  $e_4$  cannot be expressed without node  $n_4$  in the network. To remedy this issue, an unselected element  $i \in (V_{21} - V')$  in Phase 1 is labeled as a dummy node in Phase 2. The revised set of target nodes is defined as  $J = V_1 \cup (V_{21} - V')$ .

#### B. Phase2: UAV Path Generation (MUAV-ph2)

Based on the UAV pre-position decision from Phase 1, Phase 2 determines optimal paths for deployed UAVs to assess the target network so as to minimize the sum of UAV operating costs.

UAV  $k \in K$  starts and ends flight from/to locations  $i \in V'$  conducting damage assessment through the traverse edge  $E$ .

$$\min \sum_{k \in K} c_k^{dep} h_k + \lambda \cdot FT, \quad (5)$$

$$s. t. x_{i,j,k} \leq h_k, \quad \forall k \in K, \quad (6)$$

$$\sum_{i:(i,j) \in E \setminus E_3} \sum_{k \in K} x_{i,j,k} \geq 1, \quad \forall j \in J, \quad (7)$$

$$\sum_{(i,j) \in E_1} x_{i,j,k} = \sum_{(j,i) \in E_3} x_{j,i,k}, \quad \forall k \in K, \quad (8)$$

$$\sum_{i:(i,u) \in E \setminus E_3} x_{i,u,k} = \sum_{j:(u,j) \in E \setminus E_3} x_{u,j,k}, \quad \forall u \in J, k \in K, \quad (9)$$

$$\sum_{k \in K} (x_{i,j,k} + x_{j,i,k}) \geq 1, \quad \forall (i,j) \in E_2, \quad (10)$$

$$\sum_{(i,j) \in E} (d_{i,j} + ST_j) x_{i,j,k} \leq B_k, \quad \forall k \in K, \quad (11)$$

$$\sum_{(i,j) \in E} (d_{i,j} + ST_j) x_{i,j,k} \leq FT, \quad \forall k \in K, \quad (12)$$

$$u_i - u_j + |J| x_{i,j,k} \leq |J| - 1, \quad \forall (i,j) \in E_2, k \in K. \quad (13)$$

In MUAV-ph2, the objective function (5) is to minimize the sum of UAV deployment costs ( $c_k^{dep}$ ) which are proportional to the number of assigned UAVs, and the scanning completion time (FT). Constraint (6) indicates which UAV is allocated for the damage assessment. Constraint (7) ensures that each UAV must cover at least one target node in the network. Constraints (8) and (9) control the flow conservation of UAVs. The total number of UAVs departing from any UAV positions is the same as the number of returning UAVs in (8), and flow-in equals flow-out for any target nodes in (9). Constraint (10) expresses that any target edge  $E_2$  must be assessed at least once by maneuvering either from  $i$  to  $j$  or the opposite. Constraint (11) ensures that every UAV flight path, including flight time and inspection on a specific node, must be bounded by its maximum flight time. Constraint (12) is to calculate the minimum task completion time by UAVs. Constraint (13) is the *MTZ sub-tour elimination constraint* that is designed to ensure a complete flight path from a departing depot to a destination [33]. Details about the vehicle routing problem and sub-tour elimination methods can be found in [33].

### C. Computational Considerations

In this section, four computational techniques are discussed to improve computational performance of MUAV-ph2 as the proposed model has a framework of multiple vehicle routing which is a proven *NP-hard* problem [34].

The first technique is to simplify the flight time constraint (11) by analyzing the constraint structure as well as UAV flows in the power network. The second one is to generate an upper bound for target coverage constraint (7). In the third approach, a preprocessing algorithm is proposed to fix the values of binary variables considering flight feasibility under the given technical specifications, and to generate coefficients for the two revised constraints. Lastly, a Lagrangian relaxation method is developed to obtain a high quality lower bound on the objective function of MUAV-ph2.

#### 1) Option 1: reformulation of flight time constraint

If any UAV is not assigned for damage assessment, then there is no need to check whether the UAV can complete a flight within the maximum flight time by constraint (11). In this case,

the left-hand-side of constraint (11) is 0, but the right-hand-side remains at a constant value. Therefore, by replacing  $B_k$  to  $B_k h_k$  in constraint (14), right-hand-side can only have a positive value when a UAV is assigned to a task. Otherwise, the value is 0 since  $h_k$  is 0.

Additionally, as variable  $h_k$  indicates whether UAV  $k$  is assigned for damage assessment, constraint (14) below can substitute constraint (6) which is essentially the same.

$$\sum_{(i,j) \in E} (d_{i,j} + ST_j) x_{i,j,k} \leq B_k h_k, \quad \forall k \in K. \quad (14)$$

#### 2) Option 2: upper bound generation for target coverage constraint

This option is designed to provide an upper bound for constraint (7). According to constraint (7), a target node must be assessed by at least one UAV, but no upper limit is set on the number of UAVs flying over the node. If we impose a tighter upper bound, it can help reduce solution space; hence it can improve convergence.

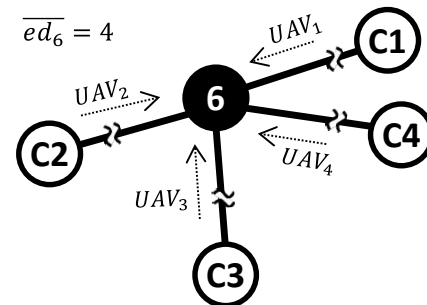


Fig. 4. An illustrative example of maximum number of UAVs passing a node

For example, as shown in Fig. 4, node 6 is connected with C1, C2, C3 and C4 over four independent edges. If each edge is scanned by multiple independent UAVs toward node 6 and flow-in to any of UAV depots off the network, then a total of four UAVs will fly over node 6. Therefore, constraint (7) can be reinforced by limiting the number of maximum allowed UAVs on node  $j$   $\overline{ed}_j$  as an upper bound shown in constraint (15). Upper bound  $\overline{ed}_j$  is obtained by Algorithm 2 discussed in Option 3 below.

$$1 \leq \sum_{i:(i,j) \in E \setminus E_3} \sum_{k \in K} x_{i,j,k} \leq \overline{ed}_j, \quad \forall j \in J. \quad (15)$$

#### 3) Option 3: probing-based preprocessing

To speed up solving MUAV-ph2 model, an efficient preprocessing algorithm is developed. First, if the flight distance between two nodes is greater than the maximum flight time of UAV  $B_k$ , then the variable  $x_{i,j,k}$  will be fixed to 0. Second, the maximum number of UAVs passing over node  $j$   $\overline{ed}_j$  is counted which set an upper bound in (15). Algorithm 2 provides an overview of the proposed probing-based preprocessing procedure.

#### Algorithm 2: A probing-based preprocessing

Initialize  $\overline{ed}_j$

```

for  $(i, j) \in E, k \in K$  do
  if  $(d_{i,j} > B_k)$  then: flight feasibility check
     $x_{i,j,k} = 0$ 
  end if
  if  $(d_{i,j} \neq 0)$  then: upper bound for (15)
     $\overline{ed}_j = \overline{ed}_j + 1$ 
  end if
end for

```

#### 4) Option 4: Lagrangian relaxation for lower bound generation

A high quality lower bound on the objective function of MUAV-ph2 can be generated utilizing Lagrangian heuristic approach. In MUAV-ph2 model, the number of sub-tour elimination constraints, i.e., (13), is exponential which can consume significant computational resources [35, 36]. Therefore constraint (13) is relaxed and added to the objective function (5) as follows:

$$\begin{aligned}
 L(\lambda) = & \min \sum_{k \in K} c_k^{dep} h_k + \lambda \cdot FT \\
 & + \sum_{k \in K} \sum_{(i,j) \in E_2} \lambda_{i,j,k} \{u_i - u_j + |x_{i,j,k} - 1| + 1\}, \quad (16) \\
 & \text{s.t. (6) - (13) where } \lambda_k \geq 0.
 \end{aligned}$$

The Lagrangian dual problem  $L(\lambda)$  provides a lower bound on the objective function of MUAV-ph2 model. From the Lagrangian dual problem, the Lagrangian multiplier is iteratively modified to find the best lower bound by using subgradient method summarized as follows:

#### Algorithm 3: Subgradient method

Initialize upper bound  $\bar{L} = \infty, \lambda_{i,j,k} \geq 0, \theta = 2$

**repeat**

$\gamma_{i,j,k} = g(x_{i,j,k}):$  gradient of  $L(\lambda_{i,j,k})$

$t_j = \frac{\theta_j (\bar{L} - L(\lambda_{i,j,k}))}{\|\gamma_{i,j,k}\|^2}:$  step size

$\lambda'_{i,j,k} = \lambda_{i,j,k}$

$\lambda_{i,j,k} = \max\{0, \lambda_{i,j,k} + t_j \gamma_{i,j,k}\}$

**until** termination condition  $\|\lambda'_{i,j,k} - \lambda_{i,j,k}\| < \varepsilon$  is satisfied

## IV. COMPUTATIONAL RESULTS

We conducted experiments for the proposed MUAV model that is composed of two phases: MUAV-ph1 (UAV pre-positioning locations) and MUAV-ph2 (UAV routing decisions).. In the first part, MUAV-ph1 is validated by using simulated random data to know how it works under extreme conditions comparing with the solutions from a deterministic model. To simulate uncertain weather condition in MUAV-ph1, the impact scale of an extreme weather  $wx_{i,j,\omega}$  is randomly generated where  $wx_{i,j,\omega} \sim U(0.4, 0.9)$ . In the second one, MUAV-ph2 is tested with a real power network in the Midwestern USA shown in Fig. 5.

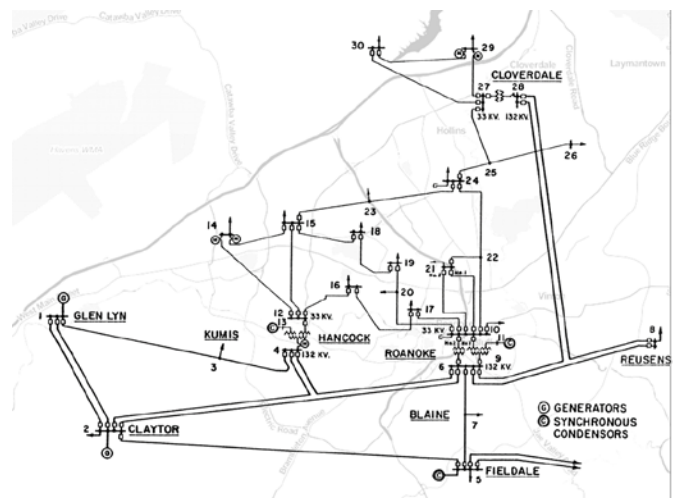


Fig. 5. Power network system example in Roanoke, VA, USA [39]

All experiments were run on a Linux server with Intel Xeon 3.00 GHz processor and 364GB RAM. CPLEX 12.6 [37] was used as the mixed integer programming (MIP) solver. We exploited the solution pool feature of CPLEX in which a group of feasible solution candidates (i.e., UAV pre-positioning locations in Phase 1 and UAV paths in Phase 2) are quickly generated to find a near optimal solution [37].

Two algorithm termination criteria are relative termination tolerance gap of 3% and 12 hours CPU run time limit, and it terminates whichever comes first.

TABLE I  
UAV FLEET SPECIFICATIONS

	Type I	Type II	Unit
Number	15	15	ea.
Max. flight time	25	35	min.
UAV unit cost	2,500	3,500	USD

Table I shows the specification of a UAV fleet that two types of UAVs are available for damage assessment. Each type of UAVs has different flight capacity and operating cost.

We evaluated the stochastic MUAV-ph1 model using the value of stochastic solution (VSS) [38]. For the calculation of VSS, the objective value of MUAV-ph1 model  $EV_{sto}$  with 50 scenarios and the expected value  $EV_{det}$  of its deterministic counterparts are compared in 10 problem instances with different problem sizes. As seen in Table II, the VSS column is obtained by subtracting the  $EV_{sto}$  column from the  $EV_{det}$  column. Considering that Phase 1 is a minimization problem, the positive VSS value supports that MUAV-ph1 under stochastic assumption outperformed the deterministic model in all cases presented in this section. Note that all test cases were solved within 1 minute of CPU time.

TABLE II  
COMPARISON OF MUAV-PH1 AND ITS DETERMINISTIC COUNTERPARTS.

Case ID	Number of nodes	$EV_{sto}$	$EV_{det}$	VSS	CPU time (sec.)
#1	20	1,980	2,500	520 (20.8%)	3.9
#2	25	1,940	2,460	520 (21.1%)	10.0
#3	30	1,900	2,500	600 (24.0%)	12.7
#4	35	1,900	2,420	520 (21.5%)	15.9
#5	40	1,780	2,340	560 (23.9%)	20.0
#6	45	1,900	2,460	560 (22.8%)	31.3
#7	50	1,860	2,500	640 (25.6%)	42.4
#8	55	1,900	2,460	560 (22.8%)	46.7
#9	60	1,860	2,380	520 (21.8%)	54.1
#10	65	1,820	2,460	640 (26.0%)	59.7

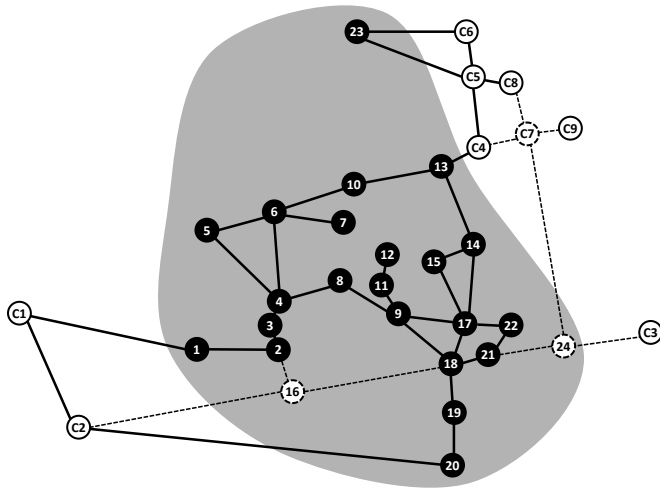


Fig. 6. Power network system topology

As a result of solving MUAV-ph1, we obtained the UAV pre-positioning locations but also identified which buses and powerlines are included in the target area. Fig. 6 shows the topology of a power network system example in Fig. 5 which is composed of 9 UAV pre-positioning locations, 30 buses, and 33 powerlines within the target area shaded in grey. Particularly, in this case, 9 dummy nodes are also included in the network for UAV path generation.

TABLE III  
UAV PATH AND TASK ASSIGNMENT

UAV ID (Type)	Power damage assessment paths ( ): node for passing purpose
#1 (I)	$C3 \rightarrow 24 \rightarrow (C7) \rightarrow C4$
#2 (I)	$C4 \rightarrow 7 \rightarrow (6) \rightarrow (4) \rightarrow 3 \rightarrow (2) \rightarrow C2$
#3 (I)	$C2 \rightarrow (16) \rightarrow 2 \rightarrow 1 \rightarrow (C1) \rightarrow C2$
#4 (I)	$C4 \rightarrow (13) \rightarrow (14) \rightarrow 15 \rightarrow 17 \rightarrow (18) \rightarrow (24) \rightarrow C3$
#5 (I)	$C4 \rightarrow (C5) \rightarrow 23 \rightarrow (C6) \rightarrow C4$
#6 (I)	$C4 \rightarrow 12 \rightarrow 11 \rightarrow 9 \rightarrow (17) \rightarrow C3$
#7 (II)	$C4 \rightarrow 13 \rightarrow 10 \rightarrow 6 \rightarrow 5 \rightarrow 4 \rightarrow C2$
#8 (II)	$C2 \rightarrow (4) \rightarrow 8 \rightarrow (9) \rightarrow (18) \rightarrow 19 \rightarrow 20 \rightarrow C2$
#9 (II)	$C4 \rightarrow 14 \rightarrow (17) \rightarrow 22 \rightarrow 21 \rightarrow 18 \rightarrow 16 \rightarrow C2$

Table III gives a MUAV-ph2 solution set that C2, C3 and C4 are minimum number of UAV positions to cover the target area. Particularly, as some target nodes, such as  $C1 \rightarrow 1$ ,  $C5 \rightarrow 23$ ,  $C6 \rightarrow 23$ , and  $C7 \rightarrow 24$  do not have a connection with selected depots, the unselected UAV pre-positioning candidates are included as dummy nodes for path generation purpose. Six

Type I UAVs and three Type II UAVs are needed to scan the target area, and assigned as the following: 2 UAVs at C2, 1 UAV at C3, and 6 UAVs at center 4.

We also conducted sensitivity analysis by varying the maximum flight time of UAV which affects to the result of MUAV-ph1 and the result of MUAV-ph2 consequently. We observed from Table IV that as maximum flight time increases, the number of depots is decreasing. In case #4, for example, if a UAV can fly up to 10 minutes, then it is possible to cover all target area only from a single depot. As a result, UAV pre-positioning setup cost is minimized but increases overall UAV operating cost in Phase 2.

TABLE IV  
UAV MAX. FLIGHT TIME AND MUAV SOLUTIONS

case no.	Max. flight time	UAV depots	UAV types	Total cost	Scanning time
#1	7 min.	<b>C2, C3, C4</b> (3)	I(6) / II(3)	$C_{dpt}^{\#1} + 255$	33.5 min.
#2	8 min.	<b>C1, C3, C4</b> (3)	I(3) / II(5)	$C_{dpt}^{\#2} + 250$	33.5 min.
#3	9 min.	<b>C1, C4</b> (2)	I(5) / II(4)	$C_{dpt}^{\#3} + 265$	33.5 min.
#4	10 min.	<b>C4</b> (1)	I(5) / II(6)	$C_{dpt}^{\#4} + 335$	34.5 min.

\* $C_{dpt}^{no}$ : UAV pre-positioning setup cost of case #no where  $C_{dpt}^{no} = \sum_{i \in V} C_i Y_i$

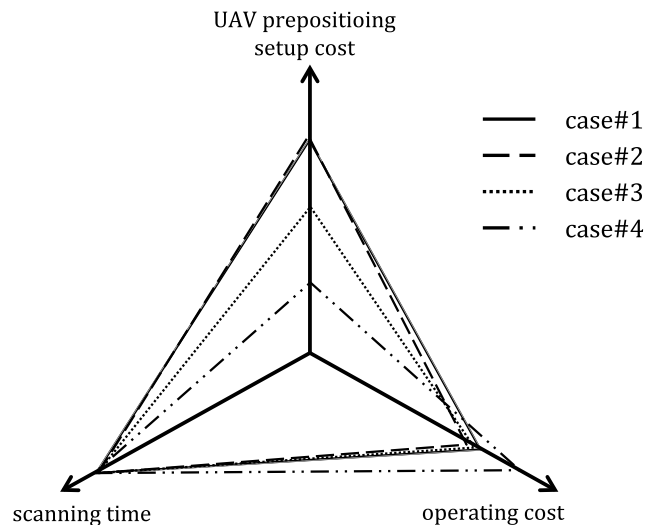


Fig. 7. Triangular relations of damage assessment time, UAV pre-positioning setup cost, and operating cost in accordance with UAV maximum flight time

As depicted in Fig. 7, UAV scanning time, pre-positioning setup cost, and operating cost have triangular relations. For example, case#2 has the least UAV operating cost comparing with other test cases. Case#4 is the most economical occasion with regards to UAV pre-positioning setup cost but has the longest scanning time.

TABLE V  
FOUR COMBINATIONS OF COMPUTATIONAL OPTIONS

Case	Option 1	Option 2	Option 3	Option 4
MUAV-ph2	No	No	No	No
MUAV_T1	Yes	No	Yes	Yes
MUAV_T2	Yes	Yes	Yes	Yes

We evaluated performance of computational techniques suggested in section III.C. For the comparison, we made three combinations of computational options as shown in Table V. MUAV-ph2 is the original MUAV model without any computational techniques. MUAV\_T1 considers 1, 3, and 4. MUAV\_T2 was solved applying every four options.

MUAV-ph2 did not converge within the 12 hours CPU run time limit and the lower bound remained at 10,021. But, both MUAV\_T1 and MUAV\_T2 found an initial feasible solution immediately with a high quality lower bound generated by the Lagrangian heuristic method. As depicted in Fig. 8, MUAV\_T2 converged faster because a tighter upper bound for target coverage constraint was provided to the model in addition to a high quality lower bound on the objective function. This confirms that these additional information to the model helps expedite convergence of the algorithm.

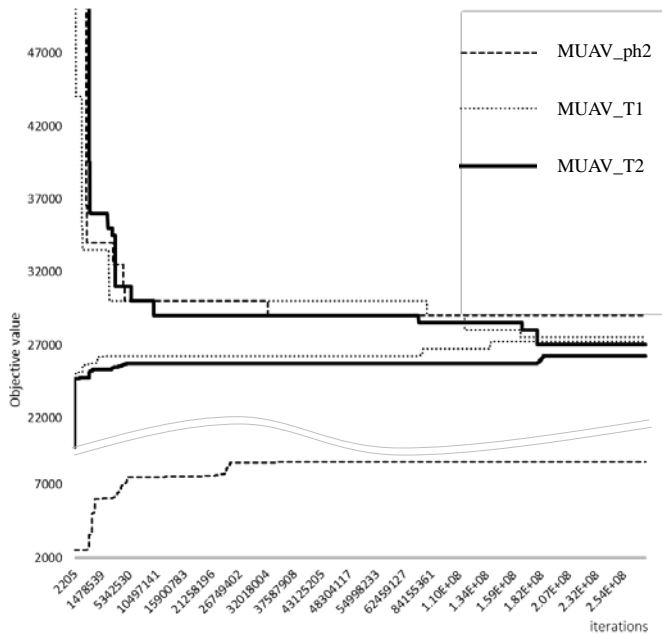


Fig. 8. Convergence

## V. CONCLUSIONS AND EXTENSIONS

A two-phase mathematical optimization model is proposed for power network damage assessment by using UAVs. As we considers uncertain weather impact to the determination of UAV pre-positioning locations, MUAV-ph1 is formulated as a two-stage stochastic program to cover a target area while minimizing total UAV positions setup cost. Based on the UAV pre-positioning locations from Phase I, MUAV-ph2 model further generated UAV paths and required number of UAVs to complete the damage assessment. As MUAV-ph2 is an NP-hard problem, we developed probing-based preprocessing techniques, a logical inequality, and also applied Lagrangian heuristic to obtain a good lower bound of MUAV-ph2 objective value in a reasonable time.

Based on experimental results, we presented the superiority of stochastic solutions comparing with deterministic solutions using VSS. By applying four computational techniques, we obtained an optimal solution in a reasonable time. Additionally, in the sensitivity analysis, triangular relations among damage assessment time, UAV pre-positioning setup cost, and operating cost were discovered by varying the service range from each UAV positions.

As an extension to this research, one can consider integrating both MUAV-ph1 and MUAV-ph2 into one model and can

provide an efficient solution strategy such as simulation-based optimization to enhance the computational performance.

## References

- [1] d. Guzman and E. M., "Eruption of Mount Pinatubo in the Philippines in June 1991," *Asian Disaster Reduction Center*, pp. 1-17, 2004.
- [2] J. Colley and a. S. M. D. Sr., "Hurricane ike impact report," Governors Office of Homeland Security, Tech. Rep, 2008.
- [3] Hodge and Neil, Allianz, December 2012. [Online]. Available: <http://www.agcs.allianz.com/insights/expert-risk-articles/energy-risks/>. [Accessed 6 February 2016].
- [4] J. Kullmann, "Electric light and power," PennWell Corporation, 2016. [Online]. Available: <http://www.elp.com/articles/print/volume-91/issue-1/sections/survey-damage-assessment-key-to-effective-outage-restoration.html>. [Accessed 13 February 2016].
- [5] Kullmann and John, "Macrosoft," 2015. [Online]. Available: <http://stage1.macrossoftindia.com/mailer/downloads/drone-article-2015.pdf>. [Accessed 1 February 2016].
- [6] W. Yuan, L. Zhao and a. B. Zeng, "Optimal power grid protection through a defender-attacker-defender model," *Reliability Engineering & System Safety*, vol. 121, pp. 83-89, 2014.
- [7] Y. Yao, T. Edmunds, D. Papageorgiou and a. R. Alvarez, "Trilevel optimization in power network defense," *IEEE Transactions on Systems, Man, and Cybernetics, Part C (Applications and Reviews)*, vol. 37, no. 4, pp. 712-718, 2007.
- [8] G. Brown, M. Carlyle, J. Salmerón and K. Wood, "Defending critical infrastructure," *Interfaces*, vol. 36, no. 6, pp. 530-544, 2006.
- [9] V. M. Bier, E. R. Gratz, N. J. Haphuriwat, W. Magua and K. R. Wierzbicki, "Methodology for identifying near-optimal interdiction strategies for a power transmission system," *Reliability Engineering & System Safety*, vol. 92, no. 9, pp. 1155-1161, 2007.
- [10] W. J. W. F. Q. C. C. K. a. B. Z. Yuan, "Robust Optimization-Based Resilient Distribution Network Planning Against Natural Disasters," *IEEE Transactions on Smart Grid*, no. 99, pp. 1-10, 2016.
- [11] R. B. S. B. mre Yamangil, "Designing Resilient Electrical Distribution Grids," in *29th Conferenec on Artificial Intelligence (AAAI 2015)*, Austin, Texas, 2015.
- [12] Jones, Dewi and G. Earp, "Requirements for aerial inspection of overhead electrical power lines," in *RPVs International Conference*, Bristol, 1996.
- [13] Ktrašnik, Jaka, F. Pernuš and a. B. Likar, "New robot for power line inspection," in *Robotics, Automation and Mechatronics, 2008 IEEE Conference*, 2008.
- [14] Montambault, Serge, J. Beaudry, K. Toussaint and N. Pouliot, "On the application of VTOL UAVs to the inspection of power utility assets," in *Applied Robotics*



for the Power Industry (CARPI), 2010 1st International Conference, 2010.

- [15] Bekmezci, Ilker, O. K. Sahingoz and Ş. Temel, "Flying ad-hoc networks (FANETs): A survey," *Ad Hoc Networks*, vol. 11, no. 3, pp. 1254-1270, 2013.
- [16] Jiang, Feng and A. L. Swindlehurst, "Optimization of UAV heading for the ground-to-air uplink," *Selected Areas in Communications, IEEE*, vol. 30, no. 5, pp. 993-1005, 2012.
- [17] Gardi, Alessandro, R. Sabatini, S. Ramasamy and T. Kistan, "Real-time trajectory optimisation models for next generation air traffic management systems," *Applied Mechanics and Materials*, vol. 629, pp. 327-332, 2014.
- [18] Alonso-Ayuso, Antonio, L. F. Escudero and F. J. Martín-Campo, "Collision avoidance in air traffic management: a mixed-integer linear optimization approach," *Intelligent Transportation Systems, IEEE Transactions*, vol. 12, no. 1, pp. 47-57, 2011.
- [19] Fu, Yanguang, M. Ding and C. Zhou, "Phase angle-encoded and quantum-behaved particle swarm optimization applied to three-dimensional route planning for UAV," *Systems, Man and Cybernetics, Part A: Systems and Humans, IEEE Transactions*, vol. 42, no. 2, pp. 511-526, 2012.
- [20] Fu, Yanguang, M. Ding, C. Zhou and a. H. Hu, "Route planning for unmanned aerial vehicle (UAV) on the sea using hybrid differential evolution and quantum-behaved particle swarm optimization," *Systems, Man, and Cybernetics: Systems, IEEE Transactions*, vol. 43, no. 6, pp. 1451-1465, 2013.
- [21] McLain, T. W. and R. W. Beard, "Coordination variables, coordination functions, and cooperative timing missions," *Journal of Guidance, Control, and Dynamics*, vol. 1, pp. 150-161, 2005.
- [22] H.-L. Choi, L. Brunet and J. P. How., "Consensus-based decentralized auctions for robust task allocation," *Robotics, IEEE Transactions*, vol. 25, no. 4, pp. 912-926, 2009.
- [23] B. Bethke, M. Valenti and J. P. How, "UAV task assignment," *Robotics & Automation Magazine, IEEE*, vol. 15, no. 1, pp. 39-44, 2008.
- [24] M. Alighanbari and J. P. How, "A robust approach to the UAV task assignment problem," *International Journal of Robust and Nonlinear Control*, vol. 18, no. 2, pp. 118-134, 2008.
- [25] J. Cho, G. Lim, T. Biobaku, S. Kim and H. Parsaei, "Safety and Security Management with Unmanned Aerial Vehicle (UAV) in Oil and Gas Industry," in *Procedia Manufacturing*, 2015.
- [26] C.-G. Lee, M. A. Epelman, C. C. White and Y. A. Bozer., "A shortest path approach to the multiple-vehicle routing problem with split pick-ups," *Transportation research part B: Methodological*, vol. 40, no. 4, pp. 265-284, 1999.
- [27] Y. Chan, W. B. Carter and M. D. Burnes, "A multiple-depot, multiple-vehicle, location-routing problem with stochastically processed demands," *Computers & Operations Research*, vol. 28, no. 8, pp. 803-826, 2001.
- [28] B. R and V. H. P., "A two-stage hybrid algorithm for pickup and delivery vehicle routing problems with time windows," *Computers & Operations Research*, vol. 33, no. 4, pp. 875-893, 2006.
- [29] J. Cho, G. J. Lim, T. Biobaku, S. Bora and H. Parsaei, "Liquefied Natural Gas Ship Route Planning Model Considering Market Trend Change," *Transactions on Maritime Science*, vol. 3, no. 2, pp. 119-130, 2014.
- [30] I. Maza and a. A. Ollero, "Multiple UAV cooperative searching operation using polygon area decomposition and efficient coverage algorithms," *Distributed Autonomous Robotic Systems*, vol. 6, pp. 221-230, 2007.
- [31] E. JJ, F. E, S. K and B. F, "On multiple UAV routing with stochastic targets: Performance bounds and algorithms," in *AIAA Guidance, Navigation, and Control Conference and Exhibit*, San Francisco, 2005.
- [32] M. L. Fisher, "The Lagrangian relaxation method for solving integer programming problems," *Management Science*, vol. 50, no. 12, pp. 1861-1871, 2004.
- [33] T. A. Z. R. Miller CE, "Integer programming formulation of traveling salesman problems," *Journal of the ACM (JACM)*, vol. 7, no. 4, pp. 326-329, 1960.
- [34] J. K. Lenstra and A. H. G. Kan., "Complexity of vehicle routing and scheduling problems. Networks," *Networks*, vol. 11, no. 2, pp. 221-227, 1981.
- [35] Padberg, Manfred and G. Rinaldi, "A branch-and-cut algorithm for the resolution of large-scale symmetric traveling salesman problems," *SIAM review*, vol. 33, no. 1, pp. 60-100, 1991.
- [36] L. A. Wolsey, "10. Lagrangian Duality," in *Integer programming*, New York, Wiley, 1998, pp. 167-181.
- [37] IBM, "CPLEX Optimizer," IBM, 2014. [Online]. Available: <http://www.cplex.com>. [Accessed 15 Feb 2016].
- [38] J. R. Birge and a. F. Louveaux, Introduction to stochastic programmin, Birge, J.R. and Louveaux, F., 2011. Introduction to stochastic programming. Springer Science & Business Media, 2011.
- [39] R. Christie, "Power Systems Test Case Archive," University of Washington, August 1993. [Online]. Available: [https://www.ee.washington.edu/research/pstca/pf30/pg\\_tca30fig.htm](https://www.ee.washington.edu/research/pstca/pf30/pg_tca30fig.htm). [Accessed 15 January 2016].

**GINO LIM** is Professor and Chairman in Industrial Engineering Department at the University of Houston. He holds a Ph.D. in Industrial Engineering from the University of Wisconsin-Madison. He has a keen interest in developing optimization techniques for solving large scale decision making problems in areas such as medicine, biology, network resiliency,

supply chain under disruption and transportation networks. His current research projects include Radiation Treatment Planning optimization, robust optimization in Transportation Problems, Port Security, Operating Room Scheduling. His e-mail address is [ginolim@uh.edu](mailto:ginolim@uh.edu).

**SEONJIN KIM** is a PhD student at the department of Industrial Engineering at the University of Houston. He holds a M.S. in industrial engineering from Texas A&M University. His email address is [seonjin64@gmail.com](mailto:seonjin64@gmail.com).

**JAERYOUNG CHO** is Assistant Professor in the Department of Industrial Engineering at Lamar University. He holds a Ph.D. in Industrial Engineering from University of Houston. His research interests lie in O.R. applications in large scale decision making problems in such areas as supply chain under disruption, transportation networks and military operations. His email address is [uncmac.rokag@gmail.com](mailto:uncmac.rokag@gmail.com).

**YIBIN GONG** is a graduate student in the Department of Industrial Engineering at the University of Houston. His email address is [yibin.gong@gmail.com](mailto:yibin.gong@gmail.com).

**AMIN KHODAEI** (SM'14) is an Associate Professor in the electrical and computer engineering department at University of Denver, Denver, CO. He received the Ph.D. degree in electrical engineering from the Illinois Institute of Technology, Chicago, in 2010 and was a visiting faculty (2010-2012) in the Robert W. Galvin Center for Electricity Innovation at Illinois Institute of Technology. Dr. Khodaei is the Technical Co-Chair of the 2018 IEEE PES T&D Conference and Exposition, Technical Co-Chair of the 2016 North American Power Symposium, and Chair of the IEEE Microgrid Taskforce. His research interests include power system operation, planning, computational economics, microgrids, and smart electricity grids. His email address is [amin.khodaei@du.edu](mailto:amin.khodaei@du.edu).